Cryst. Res. Technol. **44**, No. 10, 1139 – 1146 (2009) / **DOI** 10.1002/crat.200900445

Structure of several historic blades at nanoscale

M. Reibold[1,2], N. Pätzke[3], A. A. Levin[3], W. Kochmann[4], I. P. Shakhverdova[3], P. Paufler*[2], and D. C. Meyer[3]

[1] Triebenberg Laboratory, TU Dresden, 01062 Dresden, Germany
[2] Institut für Strukturphysik, TU Dresden, 01062 Dresden, Germany
[3] Junior Research Group Nanostrukturphysik, TU Dresden, 01062 Dresden, Germany
[4] Krüllsstr. 4b, 06766 Wolfen, Germany

Received 24 July 2009, accepted 24 August 2009
Published online 4 September 2009

Key words cementite, nanoparticles, archaeometallurgy.
PACS 61.46.Km, 68.37.Lp, 68.37.Og

Comparison of the structure of ancient Damascene steel blades at nanoscale with more recent ones - all made using crucible (wootz) technology and exhibiting ultra-high carbon content - showed for the first time a common feature. Despite different microstructures, colonies of wire- and tube-like particles with diameters of 40-50 nm have been observed with the aid of high-resolution transmission electron microscopy. Crystalline Fe_3C is the main phase forming those particles covered in numerous cases by a tube-like layer. These tubes were also found in an empty or partly - covered filled variant. To assess the strengthening capacity of cementite various models were compared. Dispersion strengthening seems the most efficient. Cutting edge qualities may be related to surface corrugations due to nanoparticles.

Dedicated to Prof. Wolfgang Neumann on the occasion of his 65th birthday

1 Introduction

In a preceding communication [1], the microstructure of five ultra-high carbon steels of ≥ 1.2 wt.% C had been investigated, samples of which were either taken from historic blades or manufactured following reports on ancient technologies. The common link between those steels is that they were made by forging crucible ingots produced in India or Central Asia, called wootz. (cf. e.g. [2-8]). As a common feature, cementite (Fe_3C) particles (abbr. Cm) predominated the microstructure, the various steels differing in shape and distribution of them only. While the nanohardness of Cm particles proved fairly constant, that of the two-phase pearlite differed markedly. In previous works [9-13], the present authors have found in one Damascus blade of the 17th century a secondary structure level. It consisted of colonies of Cm nanowires and indications of carbon nanotubes.

The aim of the present paper is to compare the same specimens as in [1] with respect to their nanostructure. They are (i) and (ii) genuine sabres of the 17th century (Z 9 and Z10), (iii) wootz from the 18th century forged in the year 2000 (AU), (iv) a Russian version of Damascus steel manufactured in 1992 (BU), and (v) synthetic wootz prepared by one of us (W.K.) and forged by the German blacksmith H. Denig (KO10). For further details of the genealogy of the specimens and of their treatment see [1]. For the results concerning Z10 the reader is referred to [9-13]. They will not be repeated here.

2 Experimental

For transmission electron microscopy (TEM) using a Philips CM200FEG, thin foils were prepared of as-received samples with orientations parallel and perpendicular to the surface of the blade. The standard

* Corresponding author: e-mail: paufler@physik.tu-dresden.de, peter.paufler@t-online.de

preparation techniques involved mechanical grinding, mechanical dimpling and ion milling to perforation. It should be recalled that the steel samples, including Cm, were ferromagnetic at room temperature. This may have had an impact upon quantitative results of high resolution TEM (HRTEM).

3 Results

We will report on characteristic features of each steel in turn.

Zschokke (Z 9) It is one of the two genuine Damascus sabres, which had already been studied metallographically by Zschokke [14]. Samples taken perpendicular to the blade surface as well as those perpendicular to the cross section of the sabre showed components of a nanostructure which appear like worms or socks (Fig. 1a-c) and rods or wires (Fig. 2).

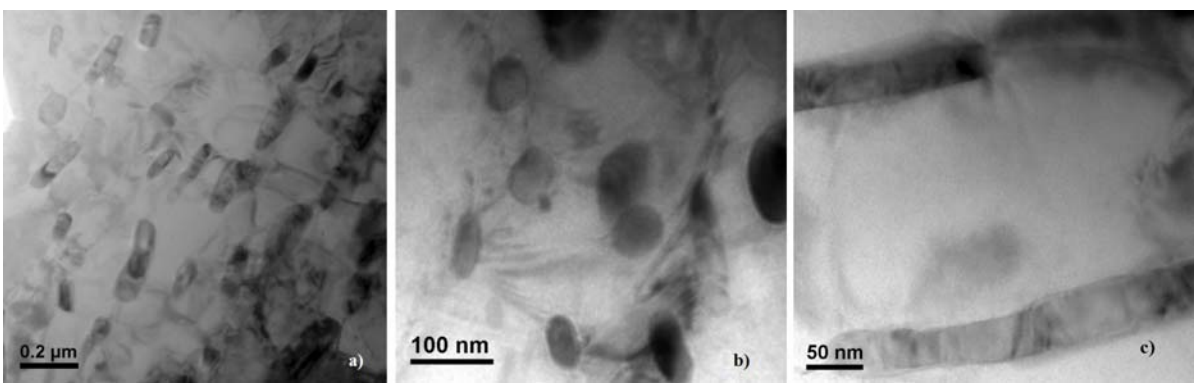

Fig. 1 Bright- field TEM image of a 17th century blade. (a) Nanoparticles in specimen Z9 approximately parallel to the blade surface. (b) Other area showing preferably the cross section of the particles. (a) and (b) are projections perpendicular to the blade surface. (c) As in (a), but enlarged view.

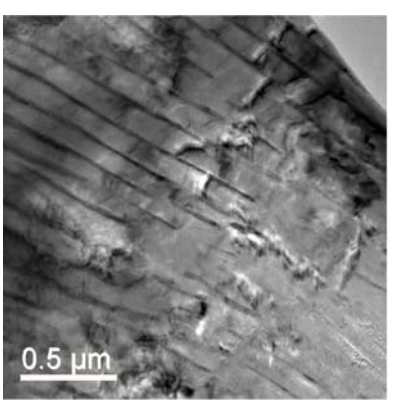

Fig. 2 Colony of almost parallel wirelike particles viewed perpendicular to the cross section of the sabre Z9.

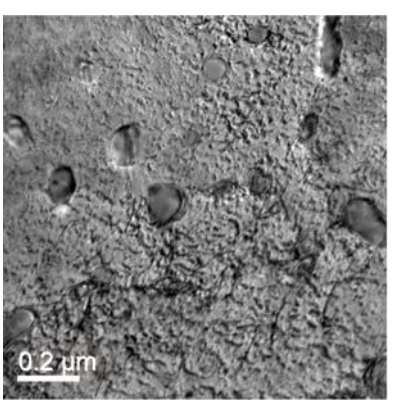

Fig. 3 TEM view of sections of various nanowires (specimen Z 9). They are arranged parallel to a plane almost horizontal and normal to the image plane. In the lower part of the image dark dislocation lines appear, indicating that wires are obstacles against dislocation movement.

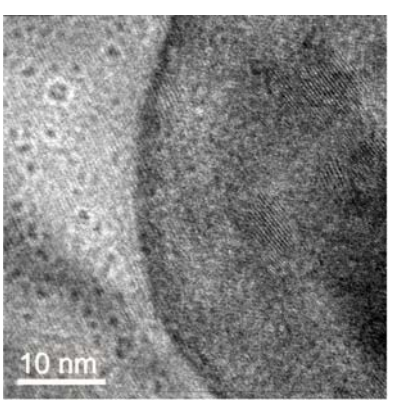

Fig. 4 Boundary between a Cm nanowire (right) and ferrite matrix (left) in Z9. Fringes confined inside the dark area indicate Fe_3C structure.

Wires often assemble in colonies. They are almost parallel and planar (Figs. 2 and 3). Features of the geometry are summarised in table 1. Using HRTEM, the internal wire structure proved cementite-like (Fig. 4). In figure 4 the boundary Cm/ferrite appeared as a dark layer, which we attribute to a carbon layer. This is supported by a dissolution experiment of the sabre in HCl reported by Reibold et al. [12]. They found similar

nanoparticles resistant against dissolution, whereas pure Cm should be solved. Hence looking at the changing contrast along the axis of these wire-like particles we interpret them as carbon tubes partly filled with Cm (Fig. 2). There are indications that Cm nanowires have been deformed plastically (Fig. 5). Inoue et al. [15] have observed slip in Fe_3C along (100)[010], (010)[001], and (001)[010], where [001] is the shortest lattice translation vector. This agrees with the slip bands activated in figure 5 where large slip steps are along (010) planes.

Augustin (AU) This sample stands for a blade manufactured from ancient wootz and forged recently. Similar wire-like contrasts were observed as in Z9. The nanowires are partly longer than those of Z9 (Fig. 6, Table 1) and appear in parts like empty tubes indicated by the uninterrupted background (Fig. 7). Locally, severe lattice distortions and hence stresses have been observed giving rise to a moiré pattern (Fig. 8).

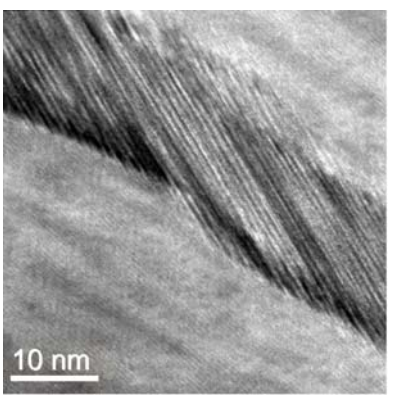

Fig. 5 HRTEM image of a Cm nanowire plastically deformed after formation in specimen Z9. Shear is along (010) planes. Fringe spacing 0.69 nm.

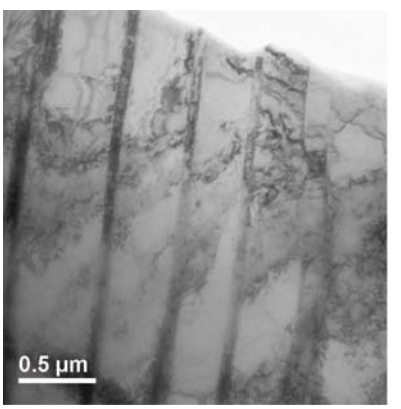

Fig. 6 Nanowires in AU.

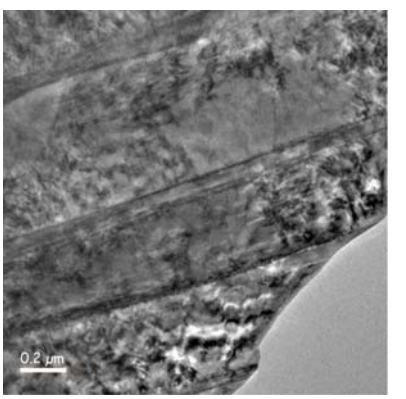

Fig. 7 Empty sections of tubes. In the background numerous dislocations appear.

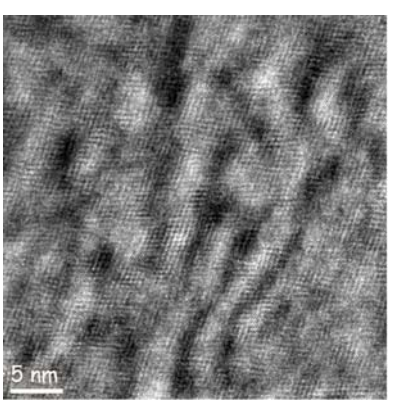

Fig. 8 HRTEM image of AU showing severe lattice distortions.

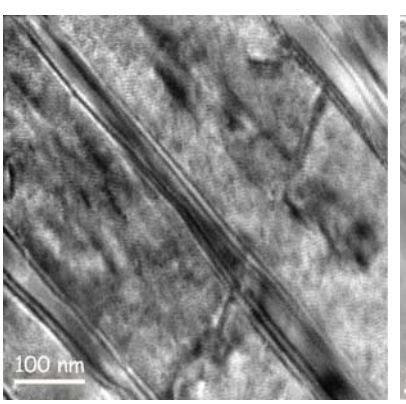

Fig. 9 TEM image displaying the nanostructure of synthetic wootz KO10. Note the double-walled contrast indicating a tilted interface between the ferrite matrix and Cm inside the stripes.

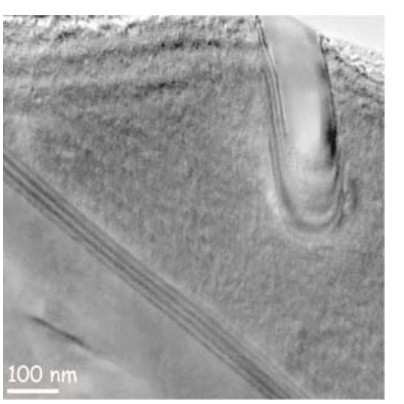

Fig. 10 Another site of KO10. A particle is ending within the image (see upper right). The ribbon crossing the image may be due to interface contrast.

Synthetic wootz (KO10) This sample stands out because the wootz was done for comparison by one of us (W.K.) and forged recently by the German blacksmith Denig. Again several examples of wire-like contrasts appeared which may have a planar interface with the matrix. (Figs. 9-11). Fig. 12 shows clearly the projection of a wire obviously bent to a spiral.

Bulat (BU) This blade was made according to the Russian tradition of Damascus steel at the end of the 20th century. A nanostructure was observed on the one hand like that of the preceding steels (linear arrays, see

Fig. 13) and showed new features on the other. Examples for the latter are sharply bounded walls around the wires (Fig. 14) and nanopores (Fig. 15).

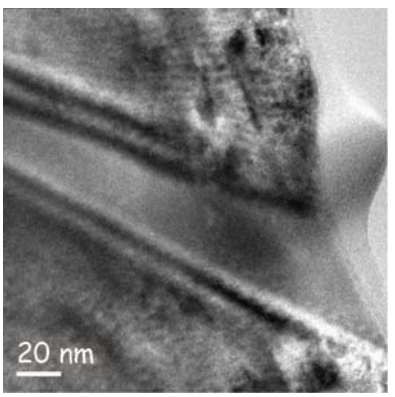

Fig. 11 Enlarged view of a wire in specimen KO10 surrounded by pronounced double wall contrast.

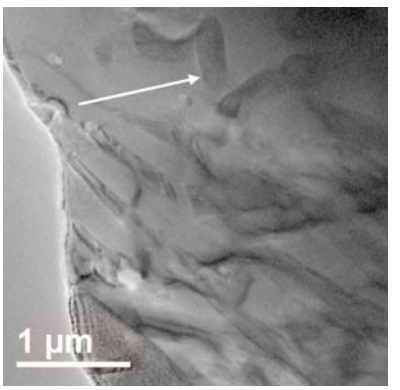

Fig. 12 TEM image of KO10. Note the wire bent helically in the upper part of the photograph (arrow).

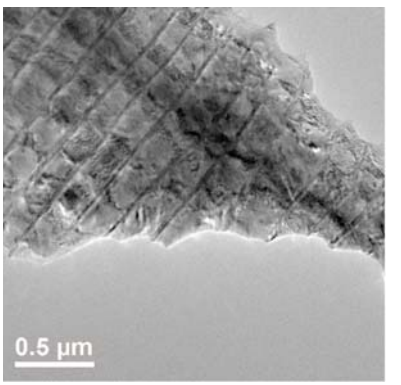

Fig. 13 TEM image of a regular array of nanowires comprises the specimen BU.

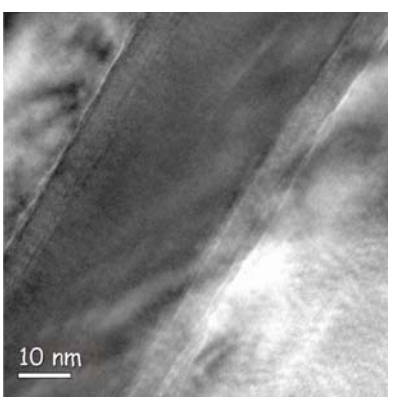

Fig. 14 A wire in the sample BU exhibiting a pronounced wall.

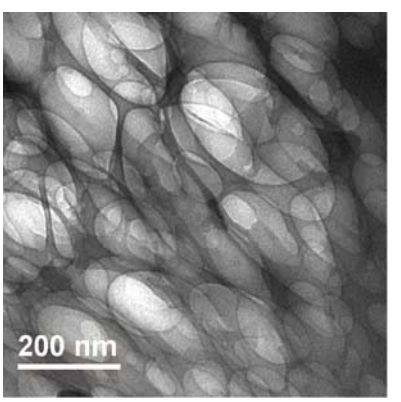

Fig. 15 TEM image showing nanopores in specimen BU.

4 Discussion

In the present work and in our previous publications on another museum-quality blade Z10 [9-13] we found colonies of nanowires of Cm and/or nanotubes, where we attributed the latter to carbon [12]. They comprised areas of some microns in diameter. In several cases wires were found inside tubes. The structure of the tubes was difficult to resolve unambiguously. Note that apart from the special case, where the sample had been dissolved in HCl [12], the tubes were always embedded in an iron-rich matrix, mostly ferrite. Hence a reaction between matrix and tube should have occurred, which presumably led to severe distortion or even amorphisation of the tube.

Since plain pearlitic steel has become known for plate-like Cm we emphasise the one-dimensional character of the nanostructure in many cases, if not in all of the specimens studied. This nanostructure cannot be recognised by optical microscopy, even more not by the naked eye. On the other hand it may have an influence upon the mechanical properties. Ferrite should have been strengthened as a nanocomposite. Note that the dimension of this structure does not vary significantly between the different steels (Table 1) which are characterised by a high carbon content of ≥.1.4 wt.%.

We will raise some points of these results. Firstly, why did previous authors fail to observe these striking objects in ancient material? The simple answer is that the resolution of previous work on ancient steel was insufficient. Moreover, material of this type is usually not readily available. As an early hint, Liu et al. [16] in a

paper on prehistoric iron from the Bacqah Valley (Jordan) identified needle-like precipitates as iron carbide. Interestingly, several authors felt that something at submicron scale should be there. Verhoeven [17,18], for example, pointed out that submicroscopic particles (possibly carbides and others) or defects could have served as preferred nucleation sites for the large Cm particles, but his TEM studies failed to display ordered arrays of them.

Table 1 Geometry of nanoparticles in ancient ultra-high carbon steels.

Specimen No.	Diameter/nm	Length/nm	Spacing/nm
Z 9_1	40-50	300-400	200
Z9_2	40	<1000	200
AU	50	>2000	400-500
KO10	50	>1000	200-250
BU	40	>2000	200-250

There are numerous reports on Cm morphology in modern alloyed steels. In many cases particles seemed plate-shaped and/or orders of magnitude larger [19-22]. Other authors found them more needle- or lath-shaped [22,23]. Also, the transition from plate-like to colonies of rod-like growth has been observed [24]. The Cm rods found by Suchomlin [22] have similar dimensions like those in the present historic material. Tiny fibres of a metastable carbide not well resolved have been observed by Pitsch et al. [25]. Also nanometre-scale carbonitride particles increasing the creep strength of martensitic steel were reported by Tanelke et al. [26]. The orientation relationship between large Cm crystals or lamellar Cm and ferrite in pearlite has been determined by a number of authors (e.g. [16,22,25,27-34]). Note that several authors use coordinate systems which may differ from the standardised space group *Pnma* adopted in the present work (i.e. convention of lattice parameters b >a >c). Some do not indicate their choice at all. We found nanoscaled Fe_3C wires with axis parallel to (010) (Fig. 16). The presence of dislocations and stacking faults was also detected directly in Cm (Fig. 16). The striking uniformity of the Cm colonies (Figs. 2, 6, 12) resembles that of Cm lamellae well known from pearlite. There are several attempts to relate this phenomenon to surface-energy, energy anisotropy and/or carbon concentration gradient arguments [24]. This may also hold here.

The small voids or pores observed in the Bulat specimen (BU) (Fig. 15) do not seem to occur in the other steels. Void formation due to dissolution of Fe_3C has been found also by Verhoeven et al.[35] after heating forged bars to about 900 °C. This may have been also the case in BU, not knowing details of the technology.

How do nanowires and nanotubes form? The precipitation of Cm from supersaturated ferrite has been modelled by Ghosh et al. [19] disregarding the impact of plastic deformation. Even if a thermodynamic reasoning for the precipitation of primary Cm can be given, an explanation of the behaviour during forging and the final formation of linear arrays of Cm had still to be found. There is evidence that carbides precipitate along dislocations thus forming regular nets [17,36]. Note that the origin of dislocations must not be restricted to forging. They could have also been created by thermal cycling as the volume change of Fe_3C due to decomposition [37] and/or thermal expansion [38] is rather large. Other authors showed that Fe_3C can be formed in the presence of metallic catalysts from CO [39] or CH_4 [40] gas. Also, carbon nanoparticles of fullerites and single layer nanotubes were detected in Fe-Ni-C alloys [41]. Authors presumed that the catalytic action of Ni lead to decomposition of hydrocarbons. So, Cm at nanoscale could alternatively be formed locally by decomposition of gases. Finally, attention has been paid to the impact of transition element impurities upon the formation of Cm. When reproducing Damascus steel, Verhoeven et al. [42] found a correlation between vanadium content and Cm particle appearance. Also Han et al. [20] concluded that vanadium may strengthen ferrite in high-carbon pearlitic steels by forming very small clusters with carbon.

There are early reports claiming that the carbon content of the high-carbon steel was achieved by combining low-carbon iron with plant matter in the crucible, i.e. in particular with hydrocarbons [2,6(p.72), 8,43-48]. Goodell et al. [49] succeeded in producing carbon nanotubes using natural fibres. So, there are two sources of C in those ancient crucible steels: Elemental C (added as coke or charcoal for example) and CH_x or CO.

All steels investigated can be considered nanocomposites consisting of a ferrite matrix and Cm fibres. The effect of nanowires, which resemble semi-coherent precipitates, upon the strength may be assessed by considering two mechanisms. The first is fibre strengthening, where the wires serve as load bearing component. Since Young's moduli of α-iron (211 GPa [50]) and Cm (194 GPa [1]) are of the same order, it is the fracture strength of Cm, σ_{Cm} = 6±2GPa [21], which predominates the strength of the composite, σ_c,

according to $\sigma_c = v_{Cm}\sigma_{Cm} + (1- v_{Cm})\ \sigma_\alpha$. Taking the fracture strength of ferrite $\sigma_\alpha = 0.045$ GPa [51] and the volume fraction of Cm, $v_{Cm} \approx 0.2$, we end up with $\sigma_c = 1.2 \pm 0.4$ GPa. The second mechanism is dispersion strengthening, where wires act as barriers to dislocation motion (see, e.g., Fig. 3). Investigating 1.8%C steel, Syn et al. [52] found empirically a Hall-Petch behaviour for the dependence of yield strength σ_y on the mean surface – to – surface particle spacing, D, and the mean ferrite grain size, L, according to $\sigma_y = 310\ (D)^{-0.5} + 460\ (L)^{-0.5}$, where σ_y is in MPa and D and L are in µm. Putting $D \approx 0.2$ µm and $L \approx 2$ µm the result is $\sigma_y = 1.0$ GPa. Note that σ_c and σ_y are of the same order. The hardness H expected from these yield stresses amounts to (3.5...2.9) GPa each, when $H \approx 2.9\ \sigma_y$ [53] is used. This agrees well with the nanohardness of the matrix of steels Z9 and Z10 (table 3 in [1]). So, we conclude that the presence of nanowires has a decisive effect upon the mechanical behaviour of these alloys. It is worth noting that Taleff et al. [54] measured flow stresses of ultra-high carbon steels at room temperature of ~ 1 GPa. Finally, we refer to our nanoscratching experiments of the matrix phase [1]. Oscillations of the lateral friction force were interpreted as due to obstacles with an average distance of 80nm. We now identify them as nanowires.

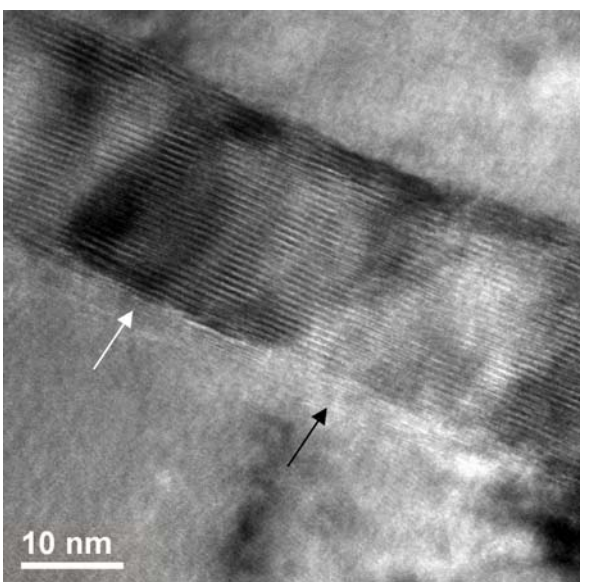

Fig. 16 In many cases the axis of Cm wires was found parallel to (010) planes as concluded from HRTEM images of the corresponding lattice planes. Note the presence of dislocations and stacking faults (arrows). Edge dislocations may not be glissile along (010) (see black arrow).

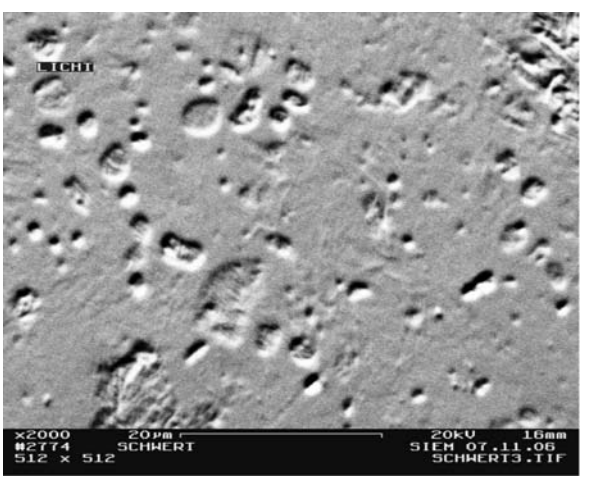

Fig. 17 Backscattered electron image of the Z10 surface registering oblique backscattering directions only (upper left). For the technique cf. [62]. Black-white rimns indicate piercing larger Cm particles. Very faint pits may indicate the place where wires penetrate. An overall grater-like surface is formed by polishing.

Even without nanowires the Cm particles known as Damast pattern generating phases give rise to a composite strengthening effect. However, the much larger particle spacing of 40-50 µm results in a yield strength more than one order of magnitude lower than that generated by nanowires.

Cm has been thought for long to behave brittle [21]. A certain degree of plasticity, however, was detected when deforming pearlitic steel [55]. In figure 5 a Cm particle embedded in a ferrite matrix underwent a change of shape by translation parallel (010) planes. Presumably, this has occurred during forging between ~750..950 °C [56,57]. This is in agreement with the finding of Keh [58], who identified (010) as the major slip and stacking fault plane of Cm. The same slip geometry has also been observed by Inoue et al. [15]. They concluded that dislocation glide along (100), (010) and (001) was connected with plastic deformation of Cm. Also, stacking faults or sequence faults parallel to (010) may have given rise to parts of the contrast of figures 5 and 16. Nishiyama et al. [59] pointed out that plane faults in Cm plates on (010) are in agreement with the structure geometry of Cm.

How did the characteristic banding of Cm come about? According to Verhoeven et al. [42] the alignment of coarse particles is the result of segregation of transition metal impurities along interdendritic regions which in turn catalyse the formation of Fe_3C. Plane bands arise after a number of forging and thermal cycling processes.

The formation of bands of coarse Cm was assumed to proceed during heating by dissolving the smaller particles and retaining the larger ones while during the cool-down period the larger would grow [18]. Since we found in the present work that nanoscaled Cm is still present in the final material simultaneously with micronscaled particles, we propose that the process is starting at nanoscale.

Damascus swords have had a legendary reputation due to their cutting quality. Several authors have attempted to explain it by referring to the microstructure. Buttin [60] drew attention to the fact that the hard Cm particles of a Damascus sword are acting like a microscopic saw when the sword or sabre is used properly (cf. [14]). A quantitative assessment of this feature, however, proved difficult [61]. Perttula concluded from experiments with leather that the blade may be superb if the Cm-rich layers locate on the ultimate cutting edge [61]. Figure 17 shows the surface of the blade of sample Zschokke 10 (Z10, cf. [9-13]) where coarse and small Cm particles pierce. It looks indeed like a grater. Wear of the surface would reproduce the pattern.

5 Conclusion

Aligned nanoscopic elongated Cm particles have been found in museum-quality wootz Damascus blades as well as in blades produced from other wootz ingots. Also, tube-like objects of the same dimension have been observed which we interpret as carbon nanotubes. Elongated Cm nanoparticles are deformed plastically thanks slip along prism planes of the orthorhombic Cm structure. Dislocations occur between Cm nanowires. Comparing various models of strengthening mechanisms of the ferrite/Cm composite let us conclude that the nanohardness is governed by the mean free path of dislocations between the nanowires. The early idea of a grater-effect of Damascus sabres has been confirmed at smaller scale.

Acknowledgements Authors are grateful to the Berne Historic Museum, to Dr. Augustin and to Mr. V. Albers for supplying the samples. They also wish to thank Mrs. Heide Müller , Dipl.-L. Hanns Toni Reiter, Mrs. Gudrun Siemroth, and Dr. Wolfgang Tirschler (TU Dresden) for help with the preparation and SEM characterisation of the samples.

References

[1] N. Pätzke, A. A. Levin, I. P. Shakhverdova, M. Reibold, W. Kochmann, P. Paufler, and D. C. Meyer, Mater. Charact. (submitted).
[2] C. Panseri, Gladius **4**, 5-66 (1965).
[3] J. Piaskowski, O Stali Damasceńskiej (PAN Wrocław, 1974).
[4] L. S. Figiel, On Damascus Steel (Atlantis Arts, Atlantis, 1991).
[5] M. Sachse, Damaszener Stahl (Stahleisen Düsseldorf, 1993) p. 67.
[6] S. Srinivasan and S. Ranganathan, India's legendary wootz steel (NIAS Bangalore, 2004).
[7] A. Feuerbach, Institute for Archaeo-Metallurgical Studies **25**, 27 (2005).
[8] A. Feuerbach, JOM **58**, 48 (2006).
[9] W. Kochmann, M. Reibold, R. Goldberg, W. Hauffe, A. A. Levin, D. C. Meyer, T. Stephan, H. Müller, A. Belger, and P. Paufler, J. Alloys Comp. **372**, L15 (2004).
[10] A. A. Levin, D. C. Meyer, M. Reibold, W. Kochmann, N. Pätzke, and P. Paufler, Cryst. Res. Technol. **40**, 905 (2005).
[11] M. Reibold, A. A. Levin, D. C. Meyer, P. Paufler, and W. Kochmann, Int. J. Mater. Res. **97**, 1172 (2006).
[12] M. Reibold, P. Paufler, A. A. Levin, W. Kochmann, N. Pätzke, and D. C. Meyer, Nature **444**, 286 (2006).
[13] M. Reibold, P. Paufler, A. A. Levin, W. Kochmann, N. Pätzke, and D. C. Meyer, in: Physics and Engineering of New Materials, Springer Proc. Physics **127**, 305 (2009).
[14] B. Zschokke, Rev. Métallurgie **21**, 639 (1924).
[15] A. Inoue, T. Ogura, and T. Masumoto, Trans Jap. Inst. Met. **17**, 149 (1976).
[16] K. H. Liu, H. Chan, M. R. Notis, and V. C. Pigott, 19th Annual Conf. Microbeam Analysis Soc., Bethlehem PA, USA, 261 (1984).
[17] J. D. Verhoeven, A. H. Pendray, and P. M. Berge, Mater. Charact. **30**, 187 (1993).
[18] J. D. Verhoeven, Steel Res. **73**, 356 (2002).
[19] G. Ghosh and G. B. Olson, Acta Mater. **50**, 2099 (2002).
[20] K. Han, D. V. Edmonds, and G. D. W. Smith, Metall Mater. Trans A **32**, 1313 (2001).
[21] W. W. Webb and W. D. Forgeng, Acta Met. **6**, 462 (1958).
[22] G. D. Suchomlin, Fiz. Met. Metallov. **42**, 965 (1976).
[23] X. Huang and N. H. Pryds, Acta Mater. **48**, 4073 (2000).

[24] K. E. Puttick, J. Iron Steel Inst. **185**, 161 (1957).
[25] W. Pitsch and A. Schrader, Archiv für das Eisenhüttenwesen **29**, 715 (1958).
[26] M. Tanelke, F. Abe, and K. Sawada, Nature **424**, 294 (2003).
[27] J. J. Trillat and S. Oketani, Acta Cryst. **5**, 469 (1952).
[28] M. Arbuzov and G. Kurdjumov, Ž. Techn. Fiz. **11**, 412 (1941).
[29] Ju. A. Bagarjackij, Dokl. Akad. Nauk SSSR **73**, 1161 (1950).
[30] P. G. Boswell and G. A. Chadwick, Scripta Metall. **11**, 1001 (1977).
[31] I. V. Isajčev, Žurn. Techn. Fiz. **17**, 835 (1947).
[32] N. J. Petch, Acta Cryst. **6**, 96 (1953).
[33] W. Pitsch, Acta Met. **10**, 79 (1962).
[34] D. S. Zhou and G. J. Shiflet, Metall. Trans. A **23**, 1259 (1992).
[35] J. D. Verhoeven, H. H. Baker, D. T. Peterson, H. F. Clark, and W. M. Yater, Mater. Charact. **24**, 205 (1990).
[36] Y. Hirotsu and S. Nagakura, Acta Metall. **20**, 645 (1972).
[37] P. Goerens, Stahl und Eisen **42**, 775 (1922).
[38] I. G. Wood, L. Vočadlo, K. S. Knight, D. P. Dobson, W. G. Marshall, G. D. Price, and J. Brodholt, J. Appl. Cryst. **37**, 82 (2004).
[39] C.-J. Choi, B.-K. Kim, O. Tolochko, and Li-Da, Rev. Adv. Mater. Sci. **5**, 487 (2003)
[40] J. Zhang and O. Ostrovski, ISIJ International **41**, 333 (2001).
[41] L. A. Chernozatonskii, V. P. Val'chuk, N. A. Kiselev, O. I. Lebedev, A. B. Ormont, and D. N. Zakharov, Carbon **35**, 749 (1997).
[42] J. D. Verhoeven, A. H. Pendray, and W. E. Dauksch, JOM **50**, 58 (1998).
[43] K. N. Rao, J. K. Mukherjee, and A. K. Lahiri, Bull Hist. Metall. Group **4**, 12 (1970).
[44] C. v. Schwarz, Stahl und Eisen **21**, 209 (1901).
[45] O. D. Sherby and J. Wadsworth, Sci. Am. **252**, 94 (1985).
[46] H. W. Voysey, J. As. Soc. Bengal **1**, 245 (1832).
[47] E. Wiedemann, Sitzungsber. Phys.-Mediz. Soz. Erlangen **43**, 114 (1911).
[48] H. Wilkinson, J. Roy. Asiatic Soc. **5**, 383 (1839).
[49] B. Goodell, X. Xinfeng, Q. Yuhui, G. Daniel, M. Peterson, J. Jellison, J. Nanosci. Nanotechnol. **8**, 2472 (2008).
[50] Smithells Metals Reference Book 8th ed., W. F. Gale and T. C. Totemeier (Eds.), (Elsevier, 2004).
[51] R. Armstrong, I. Codd, R. M. Douthwaite, and N. J. Petch, Phil. Mag. **7**, 45 (1962).
[52] C. K. Syn, D. R. Lesuer, and O. D. Sherby, Metallurg. Mater. Trans. A **25**, 1481 (1994).
[53] H. Hencky, Z. Angew. Math. Mech. **3**, 241 (1923).
[54] E. M. Taleff, C. K. Syn, D. R. Lesuer, and O. D. Sherby, Metall Mater. Trans. A **27**, 111 (1996).
[55] J. D. Embury and R. M. Fisher, Acta Met. **14**, 147 (1966).
[56] J. Piaskowski, Abhat an-Nadwa al Alamiya li-Tarih al Ulum inda 'l-Arab **1**, 238 (1978).
[57] E. M. Taleff, B. L. Bramfitt, CK. Syn, D. R. Lesuer, J. Wadsworth, and O. D. Sherby, Mater. Charact **46**, 11 (2001).
[58] A. S. Keh, Acta Met. **11**, 1101 (1963).
[59] Z. Nishiyama, A. Kor'eda, and S. Katagiri, Trans. JIM **5**, 115 (1964).
[60] Ch. Buttin, Preface to [14] p. 637.
[61] J. Perttula, Scand. J. Metallurgy **33**, 92 (2004).
[62] A. Weidner, C. Blochwitz, W. Skrotzki, and W. Tirschler, Mater. Sci. Eng. A **479**, 181 (2008).

